Experimental investigation of nodal domains in the chaotic microwave rough billiard

Nazar Savytskyy, Oleh Hul, and Leszek Sirko
Institute of Physics, Polish Academy of Sciences, Aleja Lotników 32/46, 02-668 Warszawa, Poland
(Received 7 July 2004; published 17 November 2004)

We present the results of experimental study of nodal domains of wave functions (electric field distributions) lying in the regime of Shnirelman ergodicity in the chaotic half-circular microwave rough billiard. Nodal domains are regions where a wave function has a definite sign. The wave functions Ψ_N of the rough billiard were measured up to the level number $N=435$. In this way the dependence of the number of nodal domains $\aleph_N$ on the level number N was found. We show that in the limit $N\to\infty$ a least squares fit of the experimental data reveals the asymptotic number of nodal domains $\aleph_N/N\simeq 0.058\pm 0.006$ that is close to the theoretical prediction $\aleph_N/N\simeq 0.062$. We also found that the distributions of the areas s of nodal domains and their perimeters l have power behaviors $n_s\propto s^{-\tau}$ and $n_l\propto l^{-\tau'}$, where scaling exponents are equal to $\tau=1.99\pm 0.14$ and $\tau'=2.13\pm 0.23$, respectively. These results are in a good agreement with the predictions of percolation theory. Finally, we demonstrate that for higher level numbers $N\simeq 220-435$ the signed area distribution oscillates around the theoretical limit $\Sigma_A\simeq 0.0386N^{-1}$.

DOI: 10.1103/PhysRevE.70.056209 PACS number(s): 05.45.Mt, 05.45.Df

In recent papers Blum *et al.* [1] and Bogomolny and Schmit [2] have considered the distribution of the nodal domains of real wave functions $\Psi(x,y)$ in 2D quantum systems (billiards). The condition $\Psi(x,y)=0$ determines a set of nodal lines which separate regions (nodal domains) where a wave function $\Psi(x,y)$ has opposite signs. Blum *et al.* [1] have shown that the distributions of the number of nodal domains can be used to distinguish between systems with integrable and chaotic underlying classical dynamics. In this way they provided a new criterion of quantum chaos, which is not directly related to spectral statistics. Bogomolny and Schmit [2] have shown that the distribution of nodal domains for quantum wave functions of chaotic systems is universal. In order to prove it they have proposed a very fruitful, percolationlike, model for description of properties of the nodal domains of generic chaotic system. In particular, the model predicts that the distribution of the areas s of nodal domains should have power behavior $n_s\propto s^{-\tau}$, where $\tau=187/91$ [3].

In this paper we present the first experimental investigation of nodal domains of wave functions of the chaotic microwave rough billiard. We tested experimentally some of important findings of papers by Blum *et al.* [1] and Bogomolny and Schmit [2] such as the signed area distribution Σ_A or the dependence of the number of nodal domains $\aleph_N$ on the level number N. Additionally, we checked the power dependence of nodal domain perimeters l, $n_l\propto l^{-\tau'}$, where according to percolation theory the scaling exponent $\tau'=15/7$ [3], which was not considered in the above papers.

In the experiment we used the thin (height $h=8$ mm) aluminium cavity in the shape of a rough half-circle (Fig. 1). The microwave cavity simulates the rough quantum billiard due to the equivalence between the Schrödinger equation and the Helmholtz equation [4,5]. This equivalence remains valid for frequencies less than the cutoff frequency $\nu_c=c/2h\simeq 18.7$ GHz, where c is the speed of light. The cavity sidewalls are made of 2 segments. The rough segment 1 is described by the radius function $R(\theta)=R_0+\Sigma_{m=2}^{M}a_m\times\sin(m\theta+\phi_m)$, where the mean radius $R_0=20.0$ cm, $M=20$, a_m and ϕ_m are uniformly distributed on $[0.269,0.297]$ cm and $[0,2\pi]$, respectively, and $0\leqslant\theta<\pi$. It is worth noting that following our earlier experience [6,7] we decided to use a rough half-circular cavity instead of a rough circular cavity because in this way we avoided nearly degenerate low-level eigenvalues, which could not be possible distinguished in the measurements. As we will see below, a half-circular geometry of the cavity was also very suitable in the accurate measurements of the electric field distributions inside the billiard.

The surface roughness of a billiard is characterized by the function $k(\theta)=(dR/d\theta)/R_0$. Thus for our billiard we have the angle average $\tilde{k}=(\langle k^2(\theta)\rangle_\theta)^{1/2}\simeq 0.488$. In such a billiard the dynamics is diffusive in orbital momentum due to collisions with the rough boundary because $\tilde{k}$ is much above the chaos border $k_c=M^{-5/2}=0.00056$ [8]. The roughness parameter $\tilde{k}$ determines also other properties of the billiard [9]. The

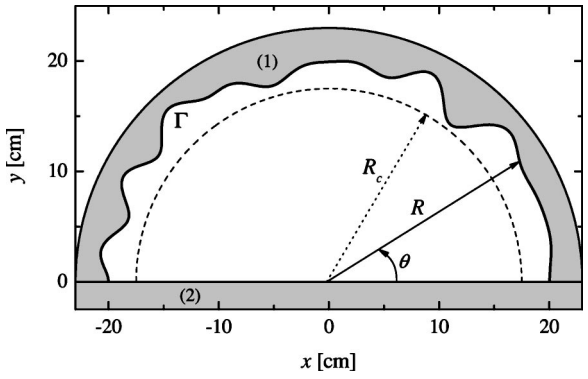

FIG. 1. Sketch of the chaotic half-circular microwave rough billiard in the xy plane. Dimensions are given in cm. The cavity sidewalls are marked by 1 and 2 (see text). Squared wave functions $|\Psi_N(R_c,\theta)|^2$ were evaluated on a half-circle of fixed radius $R_c=17.5$ cm. Billiard's rough boundary Γ is marked with the bold line.

eigenstates are localized for the level number $N < N_e = 1/128\tilde{k}^4$. Because of a large value of the roughness parameter $\tilde{k}$ the localization border lies very low, $N_e \simeq 1$. The border of Breit-Wigner regime is $N_W = M^2/48\tilde{k}^2 \simeq 35$. It means that between $N_e < N < N_W$ Wigner ergodicity [9] ought to be observed and for $N > N_W$ Shnirelman ergodicity should emerge. In 1974 Shnirelman [10] proved that quantum states in chaotic billiards become ergodic for sufficiently high level numbers. This means that for high level numbers wave functions have to be uniformly spread out in the billiards. Frahm and Shepelyansky [9] showed that in the rough billiards the transition from the exponentially localized states to the ergodic ones is more complicated and can pass through an intermediate regime of Wigner ergodicity. In this regime the wave functions are nonergodic and compose of rare strong peaks distributed over the whole energy surface. In the regime of Shnirelman ergodicity the wave functions should be distributed homogeneously on the energy surface.

In this paper we focus our attention on Shnirelman ergodicity regime.

One should mention that rough billiards and related systems are of considerable interest elsewhere, e.g., in the context of dynamic localization [11], localization in discontinuous quantum systems [12], microdisk lasers [13,14] and ballistic electron transport in microstructures [15].

In order to investigate properties of nodal domains knowledge of wave functions (electric field distributions inside the microwave billiard) is indispensable. To measure the wave functions we used a new, very effective method described in [16]. It is based on the perturbation technique and preparation of the "trial functions." Below we will describe shortly this method.

The wave functions $\Psi_N(r,\theta)$ [electric field distribution $E_N(r,\theta)$ inside the cavity] can be determined from the form of electric field $E_N(R_c,\theta)$ evaluated on a half-circle of fixed radius R_c (see Fig. 1). The first step in evaluation of $E_N(R_c,\theta)$ is measurement of $|E_N(R_c,\theta)|^2$. The perturbation technique developed in [17] and used successfully in [17–20] was implemented for this purpose. In this method a small perturber is introduced inside the cavity to alter its resonant frequency according to

$$\nu - \nu_N = \nu_N(aB_N^2 - bE_N^2), \tag{1}$$

where ν_N is the Nth resonant frequency of the unperturbed cavity, a and b are geometrical factors. Equation (1) shows that the formula cannot be used to evaluate E_N^2 until the term containing magnetic field B_N vanishes. To minimize the influence of B_N on the frequency shift $\nu - \nu_N$ a small piece of a metallic pin (3.0 mm in length and 0.25 mm in diameter) was used as a perturber. The perturber was moved by the stepper motor via the Kevlar line hidden in the groove (0.4 mm wide, 1.0 mm deep) made in the cavity's bottom wall along the half-circle R_c. Using such a perturber we had no positive frequency shifts that would exceed the uncertainty of frequency shift measurements (15 kHz). We checked that the presence of the narrow groove in the bottom wall of the cavity caused only very small changes $\delta\nu_N$ of the eigenfrequencies ν_N of the cavity $|\delta\nu_N|/\nu_N \leqslant 10^{-4}$. Therefore, its influence into the structure of the cavity's wave functions was also negligible. A big advantage of using hidden in the groove line was connected with the fact that the attached to the line perturber was always vertically positioned what is crucial in the measurements of the square of electric field E_N. To eliminate the variation of resonant frequency connected with the thermal expansion of the aluminium cavity the temperature of the cavity was stabilized with the accuracy of 0.05°.

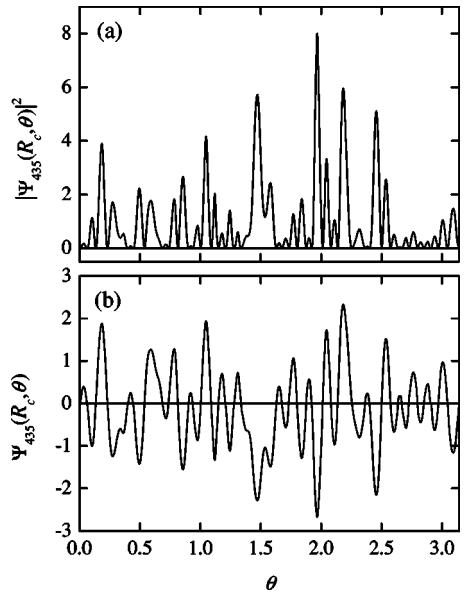

FIG. 2. Panel (a): Squared wave function $|\Psi_{435}(R_c,\theta)|^2$ (in arbitrary units) measured on a half-circle with radius $R_c = 17.5$ cm ($\nu_{435} \simeq 14.44$ GHz). Panel (b): The "trial wave function" $\Psi_{435}(R_c,\theta)$ (in arbitrary units) with the correctly assigned signs, which was used in the reconstruction of the wave function $\Psi_{435}(r,\theta)$ of the billiard (see Fig. 3). The angle θ is given in radians.

The regime of Shnirelman ergodicity for the experimental rough billiard is defined for $N > 35$. Using a field perturbation technique we measured squared wave functions $|\Psi_N(R_c,\theta)|^2$ for 156 modes within the region $80 \leqslant N \leqslant 435$. The range of corresponding eigenfrequencies was from $\nu_{80} \simeq 6.44$ GHz to $\nu_{435} \simeq 14.44$ GHz. The measurements were performed at 0.36 mm steps along a half-circle with fixed radius $R_c = 17.5$ cm. This step was small enough to reveal in details the space structure of high-lying levels. In Fig. 2(a) we show the example of the squared wave function $|\Psi_N(R_c,\theta)|^2$ evaluated for the level number $N = 435$. The perturbation method used in our measurements allows us to extract information about the wave function amplitude $|\Psi_N(R_c,\theta)|$ at any given point of the cavity but it does not allow to determine the sign of $\Psi_N(R_c,\theta)$ [21]. Our results presented in [16] suggest the following sign-assignment strategy: We begin with the identification of all close to zero minima of $|\Psi_N(R_c,\theta)|$. Then the sign "minus" maybe arbitrarily assigned to the region between the first and the second minimum, "plus" to the region between the second minimum and the third one, the next "minus" to the next region be-

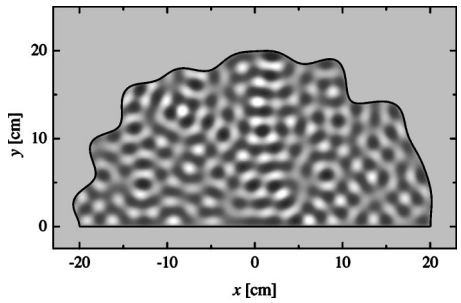

FIG. 3. The reconstructed wave function $\Psi_{435}(r,\theta)$ of the chaotic half-circular microwave rough billiard. The amplitudes have been converted into a grey scale with white corresponding to large positive and black corresponding to large negative values, respectively. Dimensions of the billiard are given in cm.

tween consecutive minima and so on. In this way we construct our "trial wave function" $\Psi_N(R_c,\theta)$. If the assignment of the signs is correct we should reconstruct the wave function $\Psi_N(r,\theta)$ inside the billiard with the boundary condition $\Psi_N(r_\Gamma,\theta_\Gamma)=0$.

The wave functions of a rough half-circular billiard may be expanded in terms of circular waves (here only odd states in expansion are considered)

$$\Psi_N(r,\theta)=\sum_{s=1}^{L} a_s C_s J_s(k_N r)\sin(s\theta), \tag{2}$$

where $C_s=[(\pi/2)\int_0^{r_{max}}|J_s(k_N r)|^2 r\,dr]^{-1/2}$ and $k_N=2\pi\nu_N/c$.

In Eq. (2) the number of basis functions is limited to $L=k_N r_{max}=l_N^{max}$, where $r_{max}=21.4$ cm is the maximum radius of the cavity. $l_N^{max}=k_N r_{max}$ is a semiclassical estimate for the maximum possible angular momentum for a given k_N. Circular waves with angular momentum $s>L$ correspond to evanescent waves and can be neglected. Coefficients a_s may be extracted from the "trial wave function" $\Psi_N(R_c,\theta)$ via

$$a_s=\left[\frac{\pi}{2}C_s J_s(k_N R_c)\right]^{-1}\int_0^{\pi}\Psi_N(R_c,\theta)\sin(s\theta)d\theta. \tag{3}$$

Since our "trial wave function" $\Psi_N(R_c,\theta)$ is only defined on a half-circle of fixed radius R_c and is not normalized we imposed normalization of the coefficients a_s: $\Sigma_{s=1}^{L}|a_s|^2=1$. Now, the coefficients a_s and Eq. (2) can be used to reconstruct the wave function $\Psi_N(r,\theta)$ of the billiard. Due to experimental uncertainties and the finite step size in the measurements of $|\Psi_N(R_c,\theta)|^2$ the wave functions $\Psi_N(r,\theta)$ are not exactly zero at the boundary Γ. As the quantitative measure of the sign assignment quality we chose the integral $\gamma\int_\Gamma|\Psi_N(r,\theta)|^2 dl$ calculated along the billiard's rough boundary Γ, where γ is length of Γ. In Fig. 2(b) we show the "trial wave function" $\Psi_{435}(R_c,\theta)$ with the correctly assigned signs, which was used in the reconstruction of the wave function

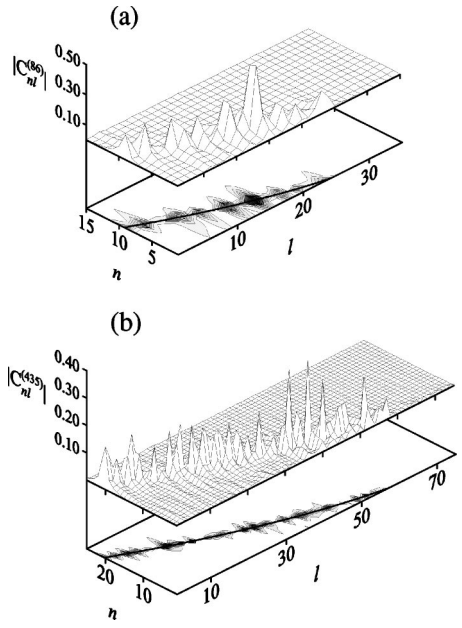

FIG. 4. Structure of the energy surface in the regime of Shnirelman ergodicity. Here we show the moduli of amplitudes $|C_{nl}^{(N)}|$ for the wave functions: (a) $N=86$; (b) $N=435$. The wave functions are delocalized in the n,l basis. Full lines show the semiclassical estimation of the energy surface (see text).

$\Psi_{435}(r,\theta)$ of the billiard (see Fig. 3). Using the method of the "trial wave function" we were able to reconstruct 138 experimental wave functions of the rough half-circular billiard with the level number N between 80 and 248 and 18 wave functions with N between 250 and 435. The wave functions were reconstructed on points of a square grid of side 4.3×10^{-4} m. The remaining wave functions from the range $N=80-435$ were not reconstructed because of the accidental near-degeneration of the neighboring states or due to the problems with the measurements of $|\Psi_N(R_c,\theta)|^2$ along a half-circle coinciding for its significant part with one of the nodal lines of $\Psi_N(r,\theta)$. These problems are getting much more severe for $N>250$. Furthermore, the computation time t_r required for reconstruction of the "trial wave function" scales like $t_r\propto 2^{n_z-2}$, where n_z is the number of identified zeros in the measured function $|\Psi_N(R_c,\theta)|$. For higher N, the computation time t_r on a standard personal computer with the processor AMD Athlon XP 1800+ often exceeds several hours, what significantly slows down the reconstruction procedure.

Ergodicity of the billiard's wave functions can be checked by finding the structure of the energy surface [8]. For this reason we extracted wave function amplitudes $C_{nl}^{(N)}=\langle n,l|N\rangle$ in the basis n,l of a half-circular billiard with radius r_{max}, where $n=1,2,3\ldots$ enumerates the zeros of the Bessel functions and $l=1,2,3\ldots$ is the angular quantum number. The moduli of amplitudes $|C_{nl}^{(N)}|$ and their projections into the energy surface for the representative experimental wave functions $N=86$ and $N=435$ are shown in Fig. 4. As expected, in the regime of Shnirelman ergodicity the wave functions are extended homogeneously over the whole energy surface [6]. The full lines on the

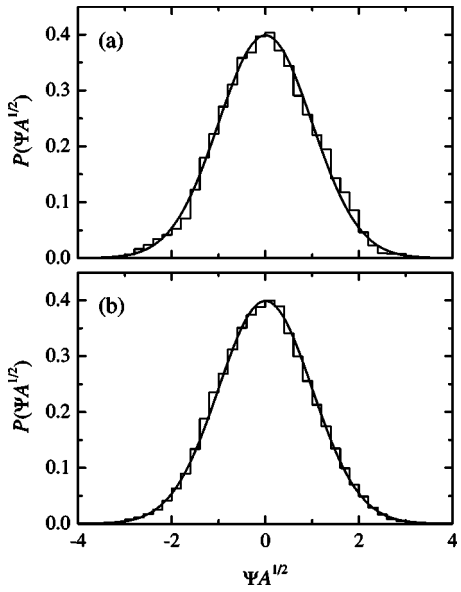

FIG. 5. Amplitude distribution $P(\Psi A^{1/2})$ for the eigenstates: (a) $N=86$ and (b) $N=435$ constructed as histograms with bin equal to 0.2. The width of the distribution $P(\Psi)$ was rescaled to unity by multiplying normalized to unity wave function by the factor $A^{1/2}$, where A denotes billiard's area. Full line shows standard normalized Gaussian prediction $P_0(\Psi A^{1/2})=(1/\sqrt{2\pi})e^{-\Psi^2 A/2}$.

projection planes in Fig. 4(a) and Fig. 4(b) mark the energy surface of a half-circular billiard $H(n,l)=E_N=k_N^2$ estimated from the semiclassical formula [7]: $\sqrt{(l_N^{max})^2-l^2}-l\arctan(l^{-1}\sqrt{(l_N^{max})^2-l^2})+\pi/4=\pi n$. The peaks $|C_{nl}^{(N)}|$ are spread almost perfectly along the lines marking the energy surface.

An additional confirmation of ergodic behavior of the measured wave functions can be also sought in the form of the amplitude distribution $P(\Psi)$ [22,23]. For irregular, chaotic states the probability of finding the value Ψ at any point inside the billiard, without knowledge of the surrounding values, should be distributed as a Gaussian, $P(\Psi)\sim e^{-\beta\Psi^2}$. It is worth noting that in the above case the spatial intensity should be distributed according to Porter-Thomas statistics [5]. The amplitude distributions $P(\Psi A^{1/2})$ for the wave functions $N=86$ and $N=435$ are shown in Fig. 5. They were constructed as normalized to unity histograms with the bin equal to 0.2. The width of the amplitude distributions $P(\Psi)$ was rescaled to unity by multiplying normalized to unity wave functions by the factor $A^{1/2}$, where A denotes billiard's area [see formula (23) in [22]]. For all measured wave functions in the regime of Shnirelman ergodicity there is a good agreement with the standard normalized Gaussian prediction $P_0(\Psi A^{1/2})=(1/\sqrt{2\pi})e^{-\Psi^2 A/2}$.

The number of nodal domains $\aleph_N$ versus the level number N in the chaotic microwave rough billiard is plotted in Fig. 6. The full line in Fig. 6 shows a least squares fit $\aleph_N=a_1N+b_1\sqrt{N}$ of the experimental data, where $a_1=0.058\pm0.006$, $b_1=1.075\pm0.088$. The coefficient $a_1=0.058\pm0.006$ coincides with the prediction of the percolation model of Bogomolny and Schmit [2] $\aleph_N/N\simeq0.062$ within the error limits. The second term in a least squares fit corresponds to a contribution of boundary domains, i.e., domains, which include the billiard boundary. Numerical calculations of Blum *et al.* [1] performed for the Sinai and stadium billiards showed that the number of boundary domains scales as the number of the boundary intersections, that is as $\sqrt{N}$. Our results clearly suggest that in the rough billiard, at low level number N, the boundary domains also significantly influence the scaling of the number of nodal domains $\aleph_N$, leading to the departure from the predicted scaling $\aleph_N\sim N$.

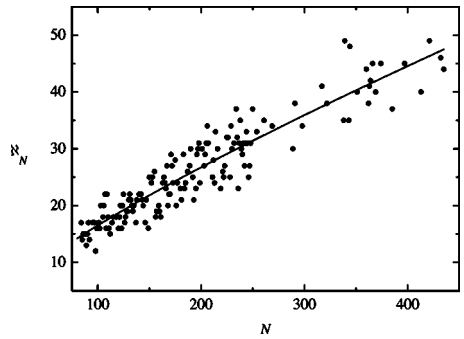

FIG. 6. The number of nodal domains $\aleph_N$ (full circles) for the chaotic half-circular microwave rough billiard. Full line shows a least squares fit $\aleph_N=a_1N+b_1\sqrt{N}$ to the experimental data (see text), where $a_1=0.058\pm0.006$ and $b_1=1.075\pm0.088$. The prediction of the theory of Bogomolny and Schmit [2] $a_1=0.062$.

The bond percolation model [2] at the critical point $p_c=1/2$ allows us to apply other results of percolation theory to the description of nodal domains of chaotic billiards. In particular, percolation theory predicts that the distributions of the areas s and the perimeters l of nodal clusters should obey the scaling behaviors: $n_s\propto s^{-\tau}$ and $n_l\propto l^{-\tau'}$, respectively. The scaling exponents [3] are found to be $\tau=187/91$ and $\tau'=15/7$. In Fig. 7 we present in logarithmic scales nodal domain areas distribution $\langle n_s/n\rangle$ versus $\langle s/s_{min}\rangle$ obtained for the microwave rough billiard. The distribution $\langle n_s/n\rangle$ was constructed as normalized to unity histogram with the bin equal to 1. The areas s of nodal domains were calculated by summing up the areas of the nearest neighboring grid sites having the same sign of the wave function. In Fig. 7 the

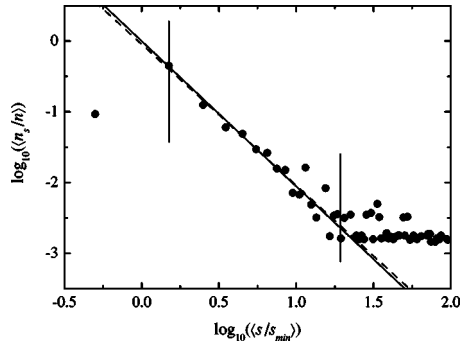

FIG. 7. Distribution of nodal domain areas. Full line shows the prediction of percolation theory $\log_{10}(\langle n_s/n\rangle)=-\frac{187}{91}\log_{10}(\langle s/s_{min}\rangle)$. A least squares fit $\log_{10}(\langle n_s/n\rangle)=a_2-\tau\log_{10}(\langle s/s_{min}\rangle)$ of the experimental results lying within the vertical lines yields the scaling exponent $\tau=1.99\pm0.14$ and $a_2=-0.05\pm0.04$. The result of the fit is shown by the dashed line.

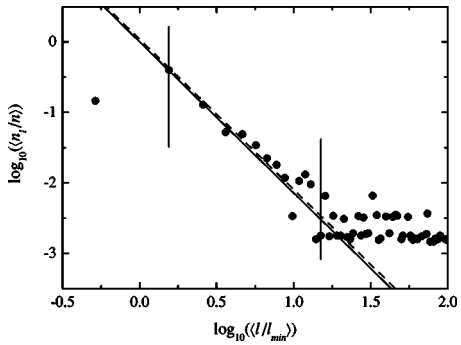

FIG. 8. Distribution of nodal domain perimeters. Full line shows the prediction of percolation theory $\log_{10}(\langle n_l/n\rangle) = -\frac{15}{7}\log_{10}(\langle l/l_{min}\rangle)$. A least squares fit $\log_{10}(\langle n_l/n\rangle) = a_3 - \tau' \log_{10}(\langle l/l_{min}\rangle)$ of the experimental results lying within the range marked by the vertical lines yields $\tau' = 2.13 \pm 0.23$ and $a_3 = 0.04 \pm 0.21$. The result of the fit is shown by the dashed line.

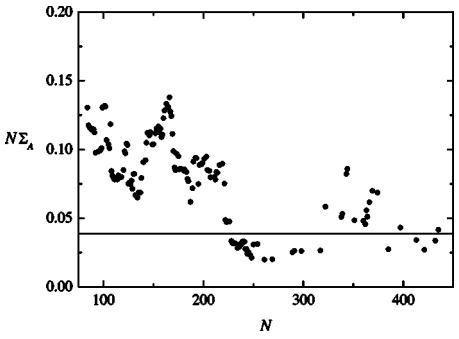

FIG. 9. The normalized signed area distribution $N\Sigma_A$ for the chaotic half-circular microwave rough billiard. Full line shows predicted by the theory asymptotic limit $N\Sigma_A \simeq 0.0386$, Blum *et al.* [1].

vertical axis $\langle n_s/n\rangle = (1/N_T)\Sigma_{i=1}^{N_T} n_s^{(N)}/n^{(N)}$ represents the number of nodal domains $n_s^{(N)}$ of size s divided by the total number of domains $n^{(N)}$ averaged over $N_T = 18$ wave functions measured in the range $250 \leqslant N \leqslant 435$. In these calculations we used only the highest measured wave functions in order to minimize the influence of bondary domains on nodal domain areas distribution. Following Bogomolny and Schmit [2], the horizontal axis is expressed in the units of the smallest possible area $s_{min}^{(N)}$, $\langle s/s_{min}\rangle = (1/N_T)\Sigma_{i=1}^{N_T} s/s_{min}^{(N)}$, where $s_{min}^{(N)} = \pi(j_{01}/k_N)^2$ and $j_{01} \simeq 2.4048$ is the first zero of the Bessel function $J_0(j_{01}) = 0$. The full line in Fig. 7 shows the prediction of percolation theory $\log_{10}(\langle n_s/n\rangle) = -187/91 \log_{10}(\langle s/s_{min}\rangle)$. In a broad range of $\log_{10}(\langle s/s_{min}\rangle)$, approximately from 0.2 to 1.3, which is marked by the two vertical lines the experimental results follow closely the theoretical prediction. Indeed, a least squares fit $\log_{10}(\langle n_s/n\rangle) = a_2 - \tau \log_{10}(\langle s/s_{min}\rangle)$ of the experimental results lying within the vertical lines yields the scaling exponent $\tau = 1.99 \pm 0.14$ and $a_2 = -0.05 \pm 0.04$, which is in a good agreement with the predicted $\tau = 187/91 \simeq 2.05$. The dashed line in Fig. 7 shows the results of the fit. In the vicinity of $\log_{10}(\langle s/s_{min}\rangle) \simeq 1$ and 1.2 small excesses of large areas are visible. A similar situation, but for larger $\log_{10}(s/s_{min}) > 4$, can be also observed in the nodal domain areas distribution presented in Fig. 5 in Ref. [2] for the random wave model. The exact cause of this behavior is not known but we can possible link it with the limited number of wave functions used for the preparation of the distribution.

Nodal domain perimeters distribution $\langle n_l/n\rangle$ versus $\langle l/l_{min}\rangle$ is shown in logarithmic scales in Fig. 8. The distribution $\langle n_l/n\rangle$ was constructed as normalized to unity histogram with the bin equal to 1. The perimeters of nodal domains l were calculated by identifying the continues paths of grid sites at the domains boundaries. The averaged values $\langle n_l/n\rangle$ and $\langle l/l_{min}\rangle$ are defined similarly as previously defined $\langle n_s/n\rangle$ and $\langle s/s_{min}\rangle$, e.g., $\langle l/l_{min}\rangle = (1/N_T)\Sigma_{i=1}^{N_T} l/l_{min}^{(N)}$, where $l_{min}^{(N)} = 2\pi\sqrt{s_{min}^{(N)}/\pi} = 2\pi(j_{01}/k_N)$ is the perimeter of the circle with the smallest possible area $s_{min}^{(N)}$. The full line in Fig. 8 shows the prediction of percolation theory $\log_{10}(\langle n_l/n\rangle) = -\frac{15}{7}\log_{10}(\langle l/l_{min}\rangle)$. Also in this case the agreement between the experimental results and the theory is good what is well seen in the range $0.2 < \log_{10}(\langle l/l_{min}\rangle) < 1.2$, which is marked by the two vertical lines. A least squares fit $\log_{10}(\langle n_l/n\rangle) = a_3 - \tau' \log_{10}(\langle l/l_{min}\rangle)$ of the experimental results lying within the marked range yields $\tau' = 2.13 \pm 0.23$ and $a_3 = 0.04 \pm 0.21$. The result of the fit is shown in Fig. 8 by the dashed line. As we see the scaling exponent $\tau' = 2.13 \pm 0.23$ is close to the exponent predicted by percolation theory $\tau' = 15/7 \simeq 2.14$. The above results clearly demonstrate that percolation theory is very useful in description of the properties of wave functions of chaotic billiards.

Another important characteristic of the chaotic billiard is the signed area distribution Σ_A introduced by Blum *et al.* [1]. The signed area distribution is defined as a variance: $\Sigma_A = \langle (A_+ - A_-)^2\rangle/A^2$, where $A_\pm$ is the total area where the wave function is positive (negative) and A is the billiard area. It is predicted [1] that the signed area distribution should converge in the asymptotic limit to $\Sigma_A \simeq 0.0386 N^{-1}$. In Fig. 9 the normalized signed area distribution $N\Sigma_A$ is shown for the microwave rough billiard. For lower states $80 \leqslant N \leqslant 250$ the points in Fig. 9 were obtained by averaging over 20 consecutive eigenstates while for higher states $N > 250$ the averaging over 5 consecutive eigenstates was applied. For low level numbers $N < 220$ the normalized distribution $N\Sigma_A$ is much above the predicted asymptotic limit, however, for $220 < N \leqslant 435$ it more closely approaches the asymptotic limit. This provides the evidence that the signed area distribution Σ_A can be used as a useful criterion of quantum chaos. A slow convergence of $N\Sigma_A$ at low level numbers N was also observed for the Sinai and stadium billiards [1]. In the case of the Sinai billiard this phenomenon was attributed to the presence of corners with sharp angles. According to Blum *et al.* [1] the effect of corners on the wave functions is mainly accentuated at low energies. The half-circular microwave rough billiard also possesses two sharp corners and they can be responsible for a similar behavior.

In summary, we measured the wave functions of the chaotic rough microwave billiard up to the level number $N = 435$. Following the results of percolationlike model proposed by [2] we confirmed that the distributions of the areas s and the perimeters l of nodal domains have power behaviors $n_s \propto s^{-\tau}$ and $n_l \propto l^{-\tau'}$, where scaling exponents are equal

to $\tau = 1.99 \pm 0.14$ and $\tau' = 2.13 \pm 0.23$, respectively. These results are in a good agreement with the predictions of percolation theory [3], which predicts $\tau = 187/91 \simeq 2.05$ and $\tau' = 15/7 \simeq 2.14$, respectively. We also showed that in the limit $N \to \infty$ a least squares fit of the experimental data yields the asymptotic number of nodal domains $\aleph_N/N \simeq 0.058 \pm 0.006$ that is close to the theoretical prediction $\aleph_N/N \simeq 0.062$ [2]. Finally, we found out that the signed area distribution Σ_A approaches for high level number N theoretically predicted asymptotic limit $0.0386N^{-1}$ [1].

This work was partially supported by KBN Grant No. 2 P03B 047 24. We would like to thank Szymon Bauch for valuable discussions.

[1] G. Blum, S. Gnutzmann, and U. Smilansky, Phys. Rev. Lett. **88**, 114101 (2002).
[2] E. Bogomolny and C. Schmit, Phys. Rev. Lett. **88**, 114102 (2002).
[3] R. M. Ziff, Phys. Rev. Lett. **56**, 545 (1986).
[4] H.-J. Stöckmann and J. Stein, Phys. Rev. Lett. **64**, 2215 (1990).
[5] H.-J. Stöckmann, *Quantum Chaos, an Introduction* (Cambridge University Press, Cambridge, England, 1999).
[6] Y. Hlushchuk, A. Błędowski, N. Savytskyy, and L. Sirko, Phys. Scr. **64**, 192 (2001).
[7] Y. Hlushchuk, L. Sirko, U. Kuhl, M. Barth, and H.-J. Stöckmann, Phys. Rev. E **63**, 046208 (2001).
[8] K.M. Frahm and D.L. Shepelyansky, Phys. Rev. Lett. **78**, 1440 (1997).
[9] K.M. Frahm and D.L. Shepelyansky, Phys. Rev. Lett. **79**, 1833 (1997).
[10] A. Shnirelman, Usp. Mat. Nauk **29**, 181 (1974).
[11] L. Sirko, Sz. Bauch, Y. Hlushchuk, P.M. Koch, R. Blümel, M. Barth, U. Kuhl, and H.-J. Stöckmann, Phys. Lett. A **266**, 331 (2000).
[12] F. Borgonovi, Phys. Rev. Lett. **80**, 4653 (1998).
[13] Y. Yamamoto and R.E. Sluster, Phys. Today **46**, 66 (1993).
[14] J.U. Nöckel and A.D. Stone, Nature (London) **385**, 45 (1997).
[15] Ya. M. Blanter, A.D. Mirlin, and B.A. Muzykantskii, Phys. Rev. Lett. **80**, 4161 (1998).
[16] N. Savytskyy and L. Sirko, Phys. Rev. E **65**, 066202 (2002).
[17] L.C. Maier and J.C. Slater, J. Appl. Phys. **23**, 68 (1952).
[18] S. Sridhar, Phys. Rev. Lett. **67**, 785 (1991).
[19] C. Dembowski, H.-D. Gräf, A. Heine, R. Hofferbert, H. Rehfeld, and A. Richter, Phys. Rev. Lett. **84**, 867 (2000).
[20] D.H. Wu, J.S.A. Bridgewater, A. Gokirmak, and S.M. Anlage, Phys. Rev. Lett. **81**, 2890 (1998).
[21] J. Stein, H.-J. Stöckmann, and U. Stoffregen, Phys. Rev. Lett. **75**, 53 (1995).
[22] S.W. McDonald and A.N. Kaufman, Phys. Rev. A **37**, 3067 (1988).
[23] M.V. Berry, J. Phys. A **10**, 2083 (1977).